DEVELOPMENT OF A METHOD FOR CALCULATING LOADS ON IMPLANTS AND PROSTHESES USED FOR THE HUMAN SKELETON

İsmet Emircan Tunç *[ID]
Gürsel Şefkat *[ID]

Abstract: The study proposes a novel computational approach for customizing sustainable knee disarticulation prostheses, aimed at improving the quality of life for users. A specialized calculation technique for assessing the loads and moments on the prosthesis was formulated, leveraging MATLAB for solving kinematic equations, Solidworks for motion analysis, and ANSYS Workbench for material and static analysis. The integration of these tools enabled the validation of the design and analytical outcomes. The kinematic solutions accounted for individual and prosthesis weights, analyzing linear and angular dynamics over a motion range pertinent to the prosthetic leg's function. Static analysis was executed to determine maximum force impact on the prosthesis. The study's results were conducive to identifying the most suitable prosthesis characteristics for individuals aged 20 to 80, with a height of 160-190 cm and a weight of 80-120 kg. The prosthetic design promoted ease of movement in activities requiring a range of motion, such as running and jumping. The prosthesis adapted swiftly to body movements, achieving readiness in approximately three seconds. The research underscores the importance of interdisciplinary collaboration between engineers and medical professionals to optimize the anatomical and kinematic aspects of prosthesis design.

Keywords: Knee Disarticulation Prosthesis, Prosthesis Modeling, Prosthetic Mechanics, MATLAB, Solidworks, ANSYS Workbench

İnsan İskeleti için Kullanılan İmplant ve Protezlere Gelen Yüklerin Hesaplanması için Bir Yöntemin Geliştirilmesi

Öz: Bu araştırma, kullanıcıların yaşam kalitesini iyileştirmeyi hedefleyen sürdürülebilir diz eksartikülasyon protezlerini kişiselleştirebilmek adına yenilikçi bir hesaplama metodolojisi önermektedir. MATLAB ile kinematik denklemlerin çözümünü, Solidworks ile hareket analizini ve ANSYS Workbench ile malzeme ve statik analizleri gerçekleştirecek şekilde özel bir hesaplama tekniği formüle edilmiştir. Bu araçların bütünleştirilmesi, tasarım ve analitik sonuçların doğrulanmasını mümkün kılmıştır. Kinematik çözümler, bireyin ve protezin ağırlıklarını dikkate alarak, protezin işlevselliğine uygun hareket aralığında lineer ve açısal dinamikleri incelemiştir. Protezin üzerindeki maksimum kuvvet etkisini belirlemek amacıyla statik analiz gerçekleştirilmiştir. Araştırmanın bulguları, 20 ile 80 yaşları arasında, 160-190 cm boy ve 80-120 kg ağırlık aralığında olan bireyler için en uygun protez özelliklerinin tespit edilmesine katkı sağlamıştır. Protez tasarımı, koşma ve zıplama gibi geniş bir hareket aralığı gerektiren aktivitelerde hareket serbestliğini desteklemiştir. Protez, vücut hareketlerine çabucak adapte olmuş ve yaklaşık üç saniye içinde kullanıma hazır duruma gelmiştir. Bu çalışma, protez tasarımının anatomik ve kinematik açılardan en iyi şekilde optimize edilmesi için mühendislik ve tıp disiplinleri arasındaki iş birliğinin kritik önemini vurgulamaktadır.

Anahtar Kelimeler: Diz eksartikülasyon Protezi, Protez Modelleme, Protez Mekaniği, MATLAB, Solidworks, ANSYS Workbench

* Department of Mechanical Engineering, Engineering Faculty, Bursa Uludağ University,16059 Nilüfer/BURSA
Corresponding Author: İsmet Emircan Tunç (ismet96.tunc@gmail.com)

1. INTRODUCTION

Joint Prosthesis Surgery, or Arthroplasty, aims to restore lost joint functions via various surgical methods (Jia et al., 2004). Prostheses can vary between the right and left legs, with transtibial prostheses and knee disarticulation prostheses being two key types (An, 2013). Primarily, transtibial prostheses serve the distances between the lower part of the kneecap and the ankle, while knee disarticulation prostheses replace the kneecap and lower leg (Anon, 2016).

There are two different application methods for these prostheses, namely external connection after shaft removal from the body and socket connection that can be worn similarly to a stocking (Tunc, 2022). Due to their functional differences - some working within the bone, others operating outside - prostheses placement must be near-perfect. This placement decision involves various factors, including the application area, the type of prosthesis, the type of surgery, and the materials used such as different Titanium alloys. Surgeons, mechanical engineers, and biomedical and biomechanical engineers collaborate to determine these procedures.

Figure 1 shows an image of the upper part of the thigh bone, or femur (AnyBody Technology, 2020). The femur, being the longest and structurally the most robust bone in mammals, is a common focus in scientific studies (Singh, 2017). The bone structure of the thigh starts broadly from the hip, narrows down towards the tibia, and then widens again (Anon,2022a).
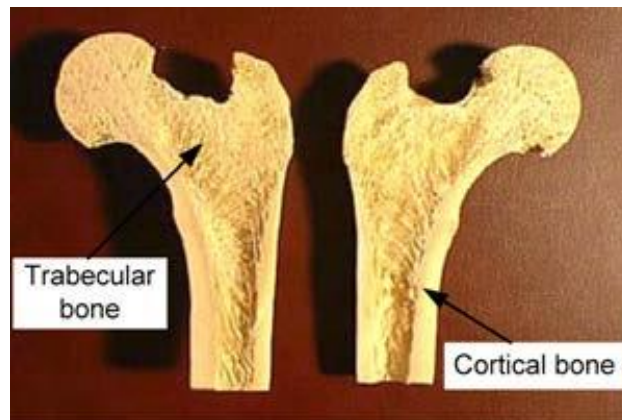
Figure 1: *Internal structure of the femur (thigh) bone. (Lei et al., 2014)*
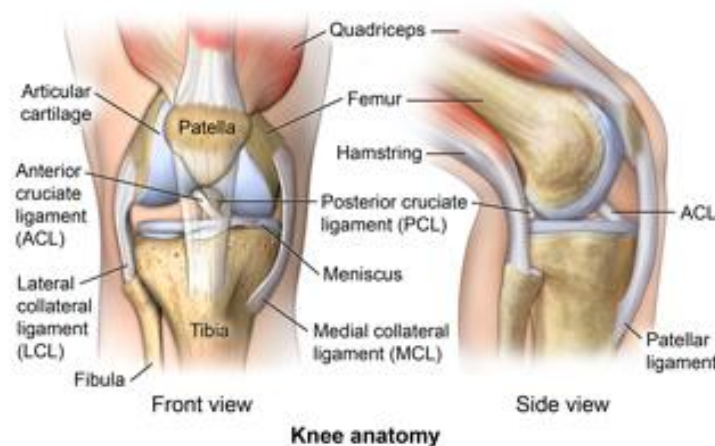
Figure 2: *Femur – tibia bone ligaments. (Anon, 2022d)*

Figure 2 illustrates the region where the femur bone ends and the tibia begins, marked by ligament structures and a cartilaginous structure (patella) nestled between these bones (Anon,2022b). This arrangement enables the transmission of hip movement to the tibia, fibula, and foot via these ligaments (Anon,2022c). The ankle joint angle gamma (γ), as shown in Figure 3, is defined as a 90° angle perpendicular to the tibia from the foot side (AnyBody Technology, 2021a).
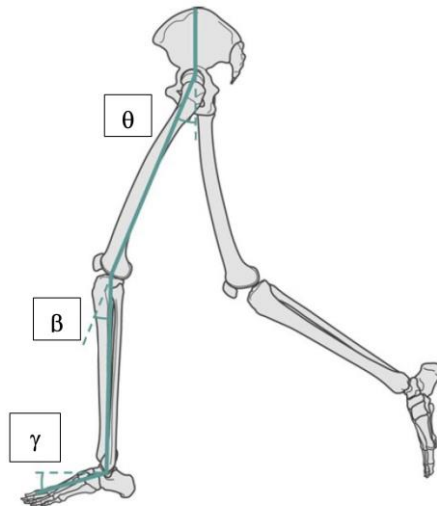
Figure 3: Joint angle definitions. (Anon, 2017)

The knee joint angle beta (β), parallel to the femur and coronal plane, is considered to be 0° and reflects angular changes aligned with the foot's reciprocating motion (Öncen, 2016). Similarly, the hip joint angle theta (θ), parallel to the coronal plane, shows angular changes according to the reciprocating motion of the foot (AnyBody Technology, 2021b).
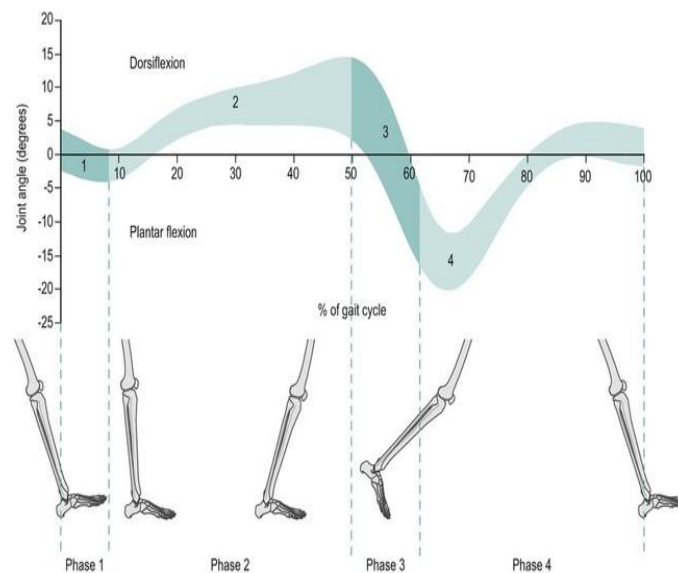
Figure 4: Ankle movement throughout the gait cycle. (Anon, 2017)

The ankle joint's movement is pivotal in the gait cycle, with the range of motion during walking varying between 20° and 40°, averaging around 30° (AnyBody Technology, 2021c). Understanding how this 30° change in ankle motion translates to the sagittal, coronal, and transverse planes throughout the gait cycle is crucial (Joseph et al., 2017). This motion has four phases during walking, each illustrated in Figure 4 (AnyBody Technology, 2021d).
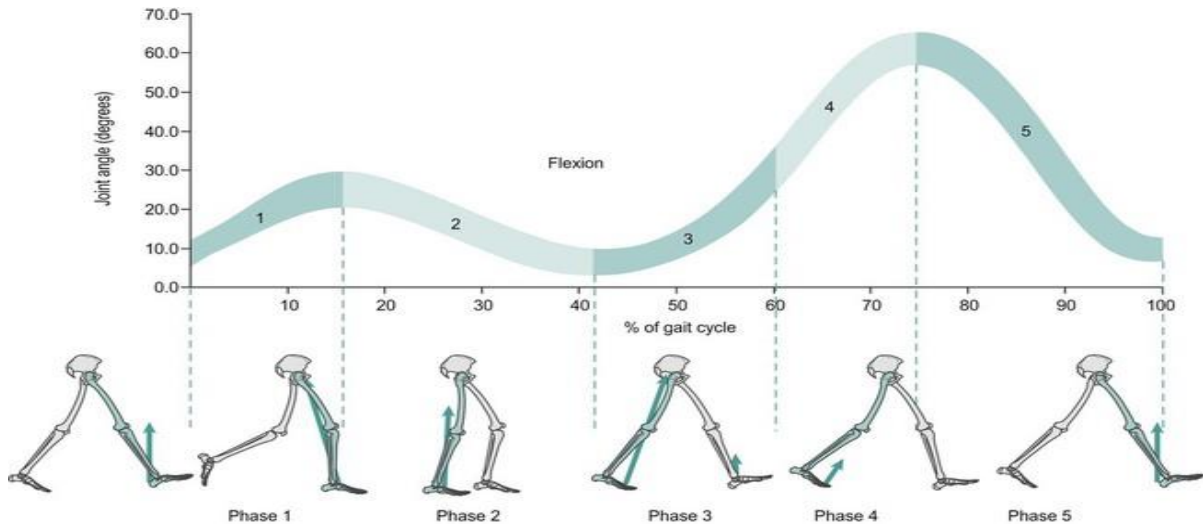
Figure 5: *Knee joint movement throughout the gait cycle. (Anon, 2017)*

The knee joint moves in the sagittal, transverse, and coronal planes while walking (Morrey, B. and Berry, D., 2011). This movement occurs in tandem with the tibia, fibula, and foot structure throughout the gait cycle. The knee joint's motion is angular and varies between 0° and 70°, and comprises five phases during walking, each depicted in Figure 5 (AnyBody Technology, 2022a). These changes further highlight the complexity and precision of movements involved in our locomotion (AnyBody Technology, 2022b).
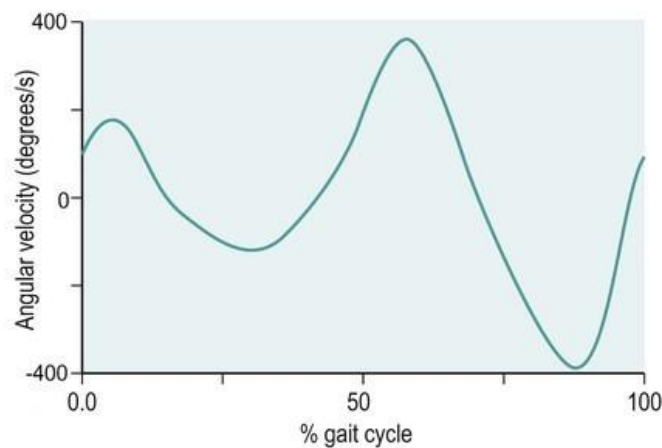
Figure 6: *Knee angular velocity during walking. (Anon, 2017)*
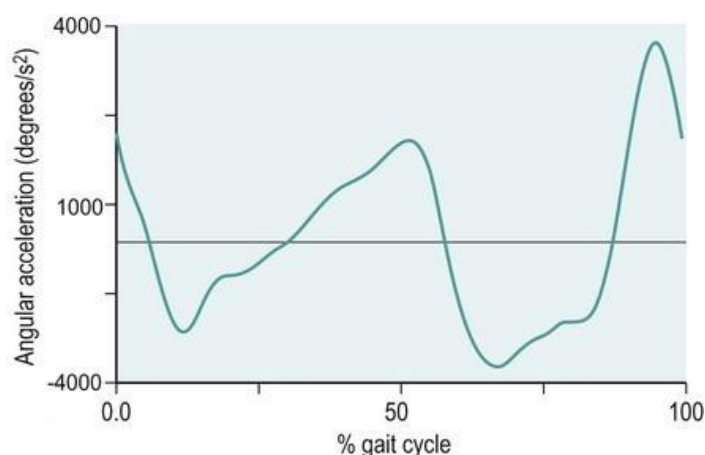
Figure 7: Knee angular acceleration during walking. (Anon, 2017)

During walking, the knee shows a steady pattern of acceleration and deceleration during the stance and swing phases. This varies depending on the movement of the oscillation. The absence of a rapid and sudden change in the acceleration values in the graph in Figure 7 shows that the movement is smooth and healthy.

Different types of knee prostheses and their applications: The study of knee prostheses has been extensive, but certain aspects require further exploration. Jia et al. (2004) provided one of the early detailed studies on knee prostheses, setting the foundational understanding of their classifications and applications. An (2013) further expanded on this, focusing on the different types of prostheses required for the right or left leg. However, as noted by Anon (2016), the literature lacks an in-depth comparative analysis of transtibial prostheses and knee disarticulation prostheses. Our study aims to address this gap by offering a comprehensive comparison of these two main types of knee prostheses.

Interdisciplinary approach in prosthetic surgeries: As rightly pointed out by Tunc (2022), the prosthetic surgery field is an intersection of multiple disciplines, including surgeons, mechanical engineers, and biomedical and biomechanical engineers. There has been a growing emphasis on the necessity for a multidisciplinary approach in these procedures, with numerous research recognizing the benefits of collaborative research (Bates, 2018; Taylor, 2019). However, the dynamics of such interdisciplinary collaboration and its impact on surgery outcomes have been largely unexplored, presenting another gap this study seeks to address.

Understanding of femur biomechanics: The femur, being the longest and one of the most structurally complex bones, has been a primary focus in biomechanical studies. Singh (2017) has provided comprehensive research on the structure and function of the femur, but more recent studies have suggested that our understanding of femur biomechanics is still incomplete (Anon, 2022a; Anon,2022b; Anon, 2022c). This study endeavors to contribute to this body of knowledge, particularly in the context of joint prosthesis surgery.

Motion mechanics of ankle and knee during gait cycle: Several studies have examined the movement of ankle and knee joints during the gait cycle (Joseph et al., 2017; Morrey & Berry, 2011). However, existing literature predominantly investigates these movements in isolation, and there is limited research on the interdependence of these movements and how variations in one may affect the other. This study aims to explore these relationships, providing a more holistic understanding of the gait cycle.

Exploring knee joint motion in different planes during walking: The multiplanar motion of the knee joint during walking has been another focus of recent research (Morrey & Berry, 2011). However, the understanding of these movements in different planes (sagittal, transverse, and coronal) and their implications for joint prosthesis surgery is still limited. This

study seeks to extend this understanding, specifically exploring the implications of knee joint movement for the application and function of knee prostheses.

However, despite extensive studies on prosthetics, there remain gaps in our understanding and challenges in their applications. One of these challenges is the differences in prostheses required for the right or left leg, which has not been addressed adequately in the literature. Further, the precise placement of the prosthesis, depending on whether it functions in the bone or outside the body, remains a subject of ongoing research. This research thus aims to address these unmet needs, offering new insights into these issues.

Moreover, the requirement for prostheses to fit near-perfectly introduces another level of complexity in prosthetic surgery. Different Titanium alloys have been used for prosthesis construction and surgery types, but the search for the most appropriate materials and surgical methods remains ongoing. The interdisciplinary nature of these procedures, involving surgeons, mechanical engineers, and biomedical and biomechanical engineers, further underscores the need for collaborative and innovative research approaches. Our work contributes to this interdisciplinary dialogue, offering a novel perspective on prosthetic application methods.

Regarding the structural analysis, the femur has been the most studied bone due to its properties and relevance in the prosthesis application. However, the biomechanics involving the transmission of movement from the hip to the tibia and fibula bone, and the foot with the help of ligaments over the femur bone, have been less explored. Similarly, the understanding of angles of the hip, knee, and ankle joints in the context of prosthesis has been limited. Our work aims to fill this gap by providing an in-depth analysis of these aspects.

The range of motion while walking varies between 20° and 40°, with an average of 30°. The importance of understanding how this 30° change in ankle motion alters in different planes throughout the gait cycle has been highlighted but not sufficiently addressed in the literature. Furthermore, the angular variation of the knee joint during walking, which varies between 0° and 70°, has been investigated, but the understanding of the five phases of this motion during the gait cycle is limited. This research focuses on addressing these specific aspects, further advancing the knowledge in this domain.

Previous studies primarily focused on examining the loads on transtibial, simple hip, and knee disarticulation prostheses. In contrast, our study utilizes accepted kinematic equations from the literature to develop an alternative calculation method. We used an innovative comparative approach with MATLAB, Solidworks, and ANSYS Workbench programs to analyze loads and moments on the prosthesis. This new approach allows us to provide personalized prostheses suitable for the individual's age, height, and weight, offering improved comfort and mobility. This study contributes to the literature by providing a new prosthetic design and validation method, highlighting the importance of collaboration between engineers and doctors for efficient prosthesis development.

2. MODELING AND RESULTS

The literature review examined loads on transtibial, simple hip, and knee disarticulation prostheses, especially for most health problems. This study decided to use the kinematic equations that are accepted and used in the literature.

This is because the study whose formulas were examined and used was made recently, and the equation is easy to analyze and calculate. Depending on the values obtained by solving the equations and then by trial-error method, the predicted age range for the prosthesis type in this study is 20-80, the expected height range is 160-190 cm, and the predicted weight range is 80-120 kg. However, the right/left-sided knee disarticulation is for a person with a prosthesis.

To contribute to the study, we conducted a six-month-long series of walking animation trials using the SolidWorks program, focusing on the prosthesis's performance. In addition, using the ANSYS Workbench program, the load on the prosthesis was calculated. Based on the 3D free

body diagram shown in Figure 8, the rotational and translational dynamic equations can be arranged as follows. (Jia et al., 2004, Castermans et al., 2014)
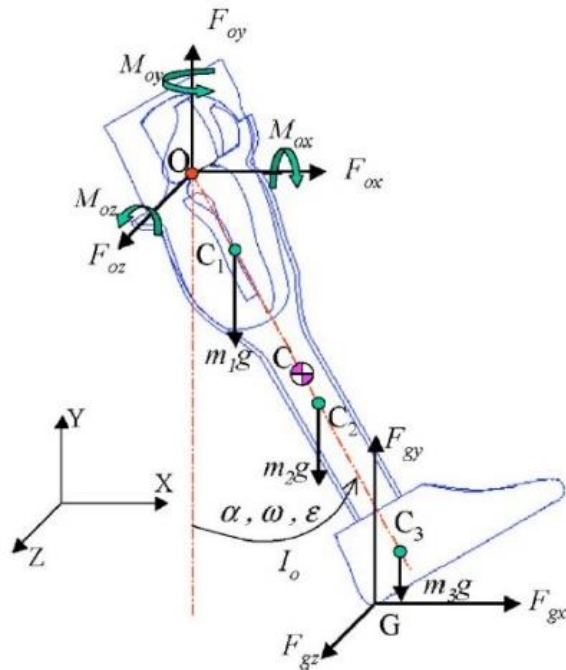
Figure 8: 3D model for calculating loads on the knee joint. (Jia et al., 2004)

$$+\circlearrowleft \sum M_z = M_{oz} - m_1 g l_1 * \sin\theta - m_2 g l_2 \sin\beta - m_3 g l_3 \sin\gamma + F_{gx} y_g + F_{gy} x_g - I_o \alpha \tag{1}$$

$$+\circlearrowleft \sum M_x = M_{ox} + F_{gy} * z_g - F_{gz} * y_g \tag{2}$$

$$+\circlearrowleft \sum M_y = M_{oy} - F_{gz} * x_g + F_{gx} * z_g \tag{3}$$

$$+\rightarrow \sum F_x = F_{ox} + F_{gx} - (m_1 + m_2 + m_3) * (r * \alpha * \cos\beta - r * \omega_x^2 * \sin\gamma) \tag{4}$$

$$+\uparrow \sum F_y = F_{oy} + F_{gy} - (m_1 + m_2 + m_3) * g - (m_1 + m_2 + m_3) \tag{5}$$
$$* (r * \alpha * \sin\beta + r * \omega_y^2 * \cos\gamma)$$

$$+\swarrow \sum F_x = F_{oz} + F_{gz} \tag{6}$$

$$r = \frac{\sum m_i * l_i}{\sum m_i} \tag{7}$$

$$I_o = m_1 * r^2 + m_2 * r^2 + m_3 * r^2 \tag{8}$$

For prosthesis modeling, m_1, m_2, and m_3 values were obtained after material assignment on Solidworks, using the body measurements of the author in this study (weight as 80 kg and height as 180 cm). Likewise, l_1, l_2, and l_3 values were obtained after assembly operations on Solidworks. The r and I_o values were calculated via the MATLAB program. $m_1 \cong 1.94$ kg, $m_2 \cong 0.91$ kg, $m_3 \cong 0.971$ kg, $l_1 = 0.29$ m, $l_2 = 0.335$ m, $l_3 \cong 0.25$ m, $r \cong 0.2905$ m and $I_o \cong 0.3217$ kgm^2.

In addition to this information, definitions of knee and ankle angles were obtained in matrix form in the MATLAB program. Angle values were given as motion input to the Solidworks program with the help of an excel file that was transposed and exported. Knee angle limits were applied to the thigh bone, and ankle borders were applied to the entire prosthesis. The definition of the angle determined in the study, which starts at -60° with an increment of 0.5° and ends at -15°, refers to the dynamic movement between the early final stance and the final swing phases according to the gait cycle. At -60°, the prosthesis oscillates, and the movement limitation requirement is completed at -15°. This movement defines the oscillating movement that allows the leg behind the body to move towards it. That can be seen in Figure 9.
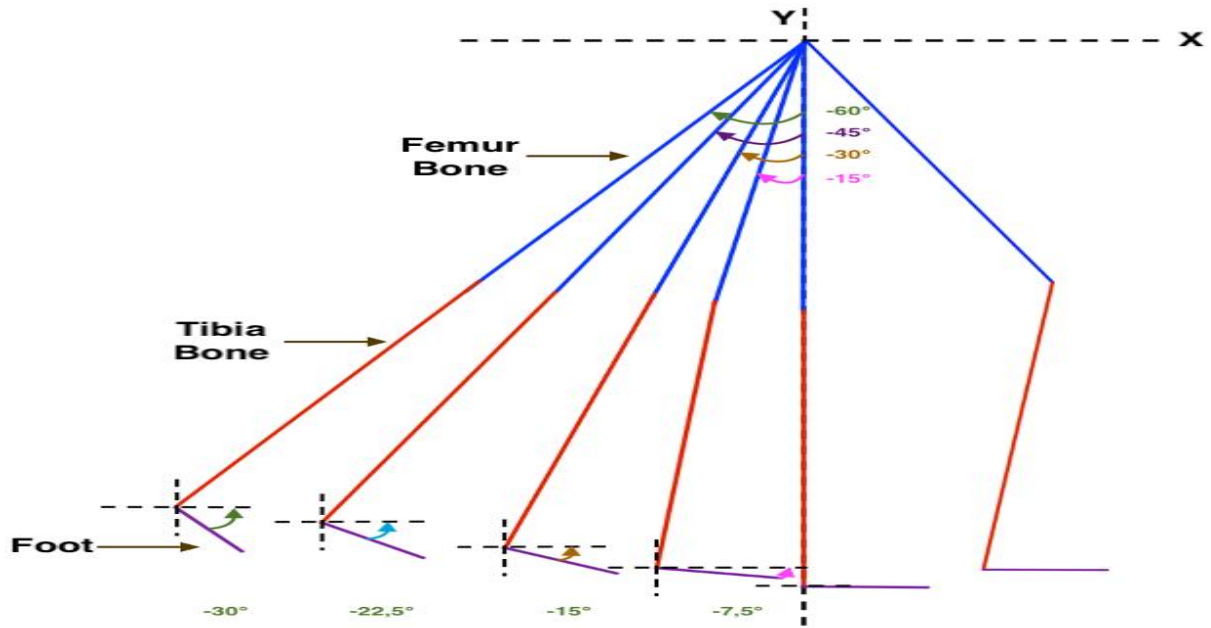
Figure 9: Leg modeling with defined motion

To find the angular velocities of the prosthesis, if the expressions ω_x and ω_y are left alone in equations 4 and 5, respectively, equations 9 and 10 will be obtained as follows.

$$\omega_x = \sqrt{(\alpha * (\cos(\beta)/\sin(\gamma)) - ((F_{ox} + F_{gx})/((m_1 + m_2 + m_3) * r * \sin(\gamma)))} \tag{9}$$

$$\omega_y = \sqrt{(F_{oy} + F_{gy})/[(m_1 + m_2 + m_3) * r * \cos(\gamma)] - (g/r * \cos(\gamma)) - (\alpha * \frac{\sin(\beta)}{\cos(\gamma)})} \tag{10}$$
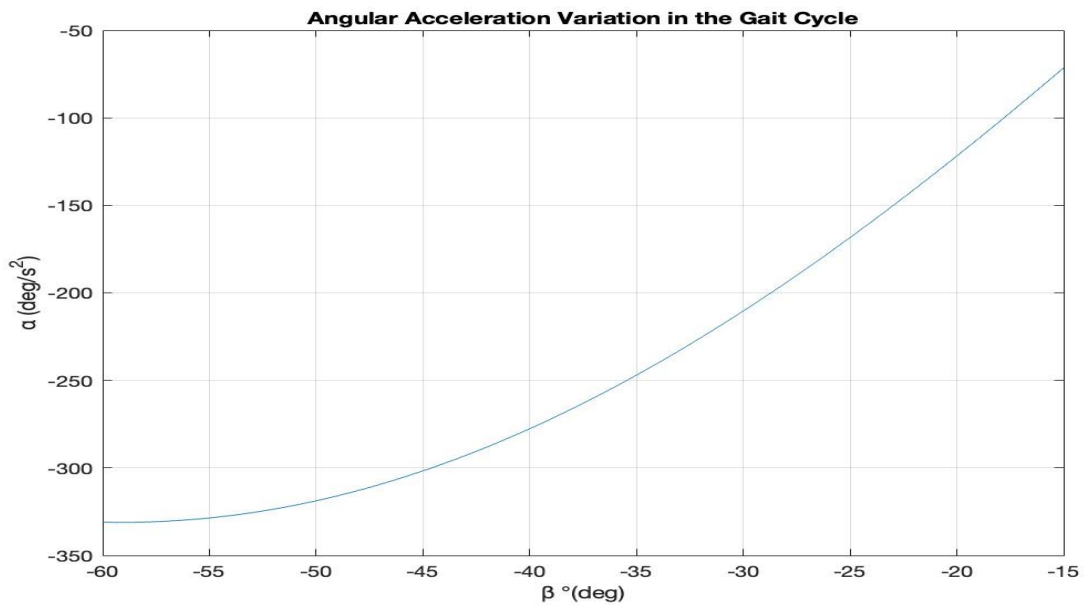
Figure 10: *Variation of angular acceleration depending on beta(β) angle from eq. (1)*

Figure 10 depicts how the angular acceleration of the prosthesis varies with the knee angle (β). As the knee angle increases, we can see a clear correlation with the angular acceleration. This graph is pivotal as it demonstrates the capability of the prosthesis to handle knee flexion and extension. The steepness of the curve, points of inflection, and other features of the graph would be essential to understand the dynamic behavior of the prosthesis under different conditions. (Garrett et al., 1999)
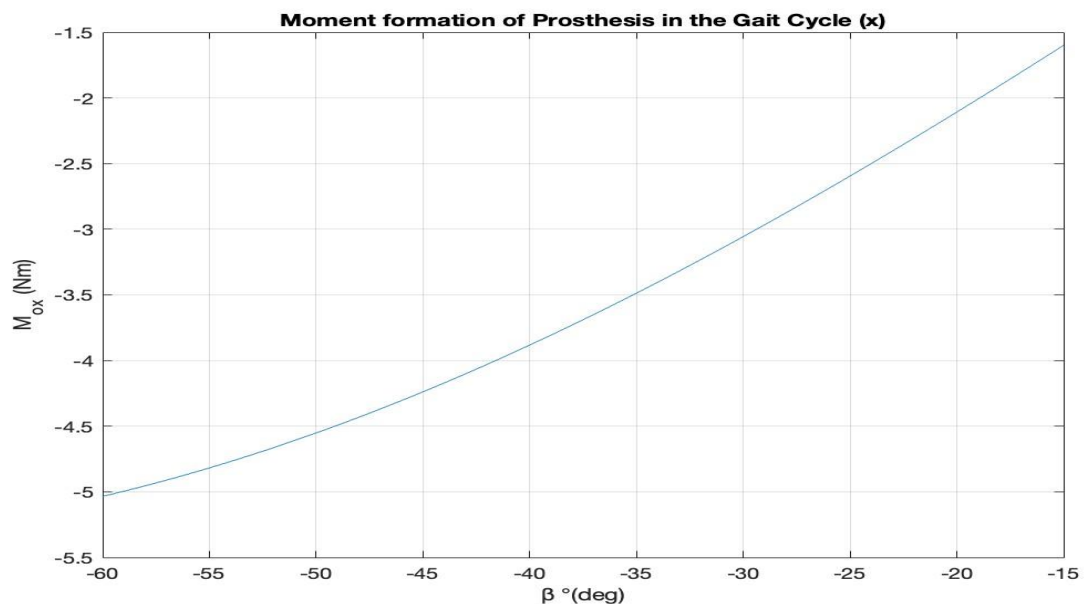
Figure 11: *The moment formation in the x direction depends on the beta(β) angle from eq. (2)*

Figure 11 examines the changing moment in the x direction, causing extension on the transverse plane. The curve showcases the moments where the prosthesis generates torque during movement. The specific pattern could reveal whether there's a moment imbalance that might affect the natural movement of the prosthesis, helping us identify areas for optimization.
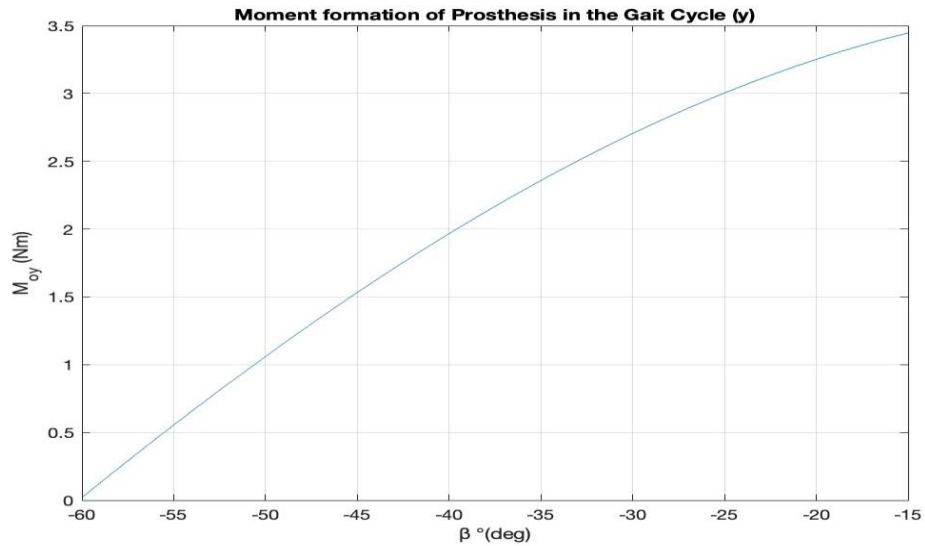
Figure 12: *The moment formation in the y direction depends on the beta(β) angle from eq. (3)*

Figure 12 displays the moment changes in the y direction that lead to abduction on the sagittal plane. The graph helps visualize how the prosthesis manages side-to-side motions. Any anomalies in the curve would suggest inefficiencies in the prosthesis's capacity to maintain a stable and comfortable gait, thereby providing key pointers for improvements.
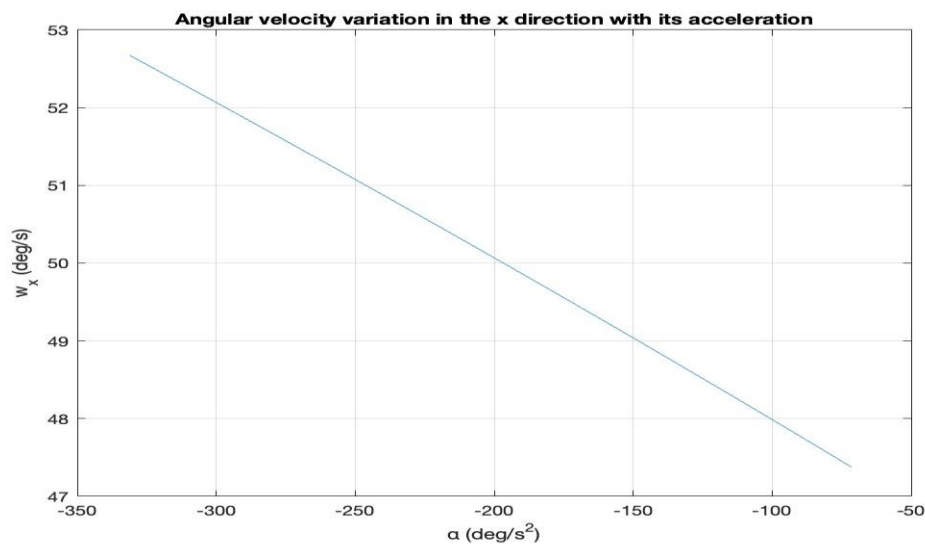
Figure 13: *Dynamic change of angular velocity in the x direction from eq. (4)*

Figure 13 traces the angular velocity variation of the x direction on the coronal plane. The graph provides a clear understanding of how velocity changes at different stages of the movement cycle. The peaks, troughs, and overall form of the graph offer a detailed look into the stability and efficiency of the prosthesis during different phases.
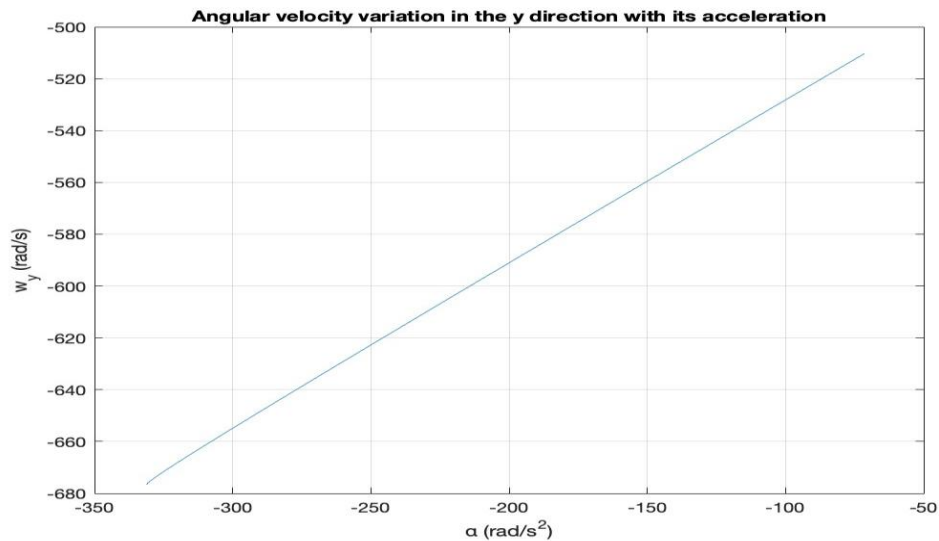
Figure 14: *Dynamic change of angular velocity in the y direction from eq. (5)*

Figure 14 details the angular velocity variation of the y direction on the coronal plane. By analyzing the data, we can observe how the prosthesis maintains a steady speed throughout the gait cycle. Any inconsistencies or irregularities in the curve would be indicative of potential areas of improvement in the prosthesis design.
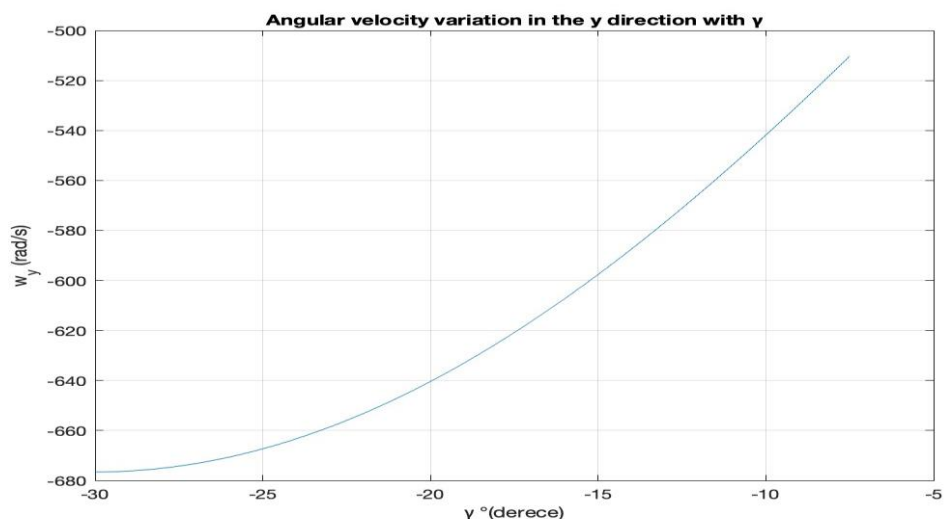
Figure 15: *Variation of angular velocity in the y direction with foot angle from eq. (5)*

Finally, Figure 15 showcases the angular velocity variation of the y direction with respect to the foot angle, which takes place on the coronal plane. This graph gives a visual representation of how changes in the foot angle affect the speed and fluidity of the prosthesis movement. This data is critical for enhancing the design and function of the prosthesis, making it more user-friendly and efficient.
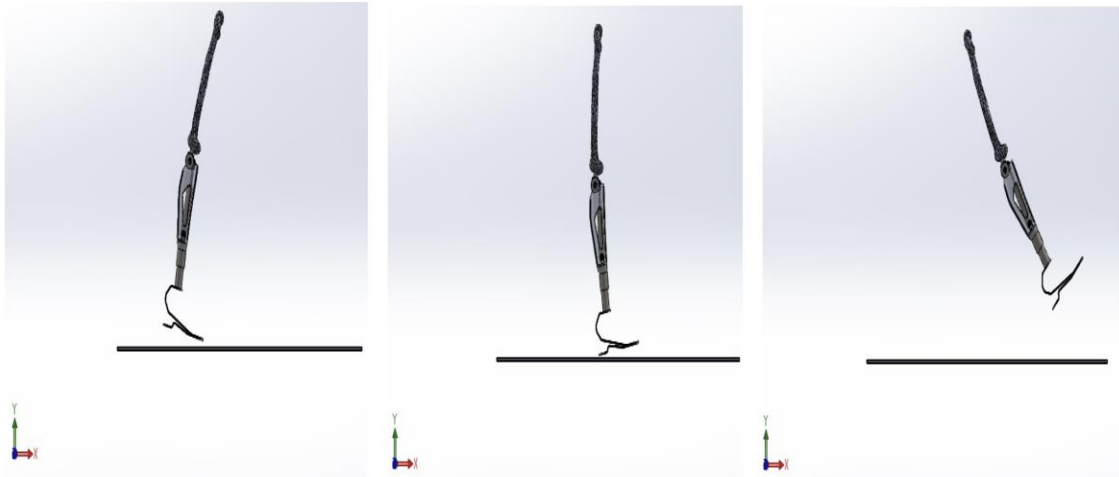
Figure 16: *Prosthesis with limited movement and a fixed increase value of 0.5° (Diogo, 2012)*

To compare the results and help understand the work, 'Motion Analysis' included the effects with the assembly in the Solidworks, as shown in figure 16. Regarding operation in motion analysis, the angular definition of -60 to 0° with 0.5° increments was defined on the femur bone and the prosthesis. The motion-limited/unbendable knee is defined in the motion analysis made here. In addition, the gravity effect is also included in the analysis.
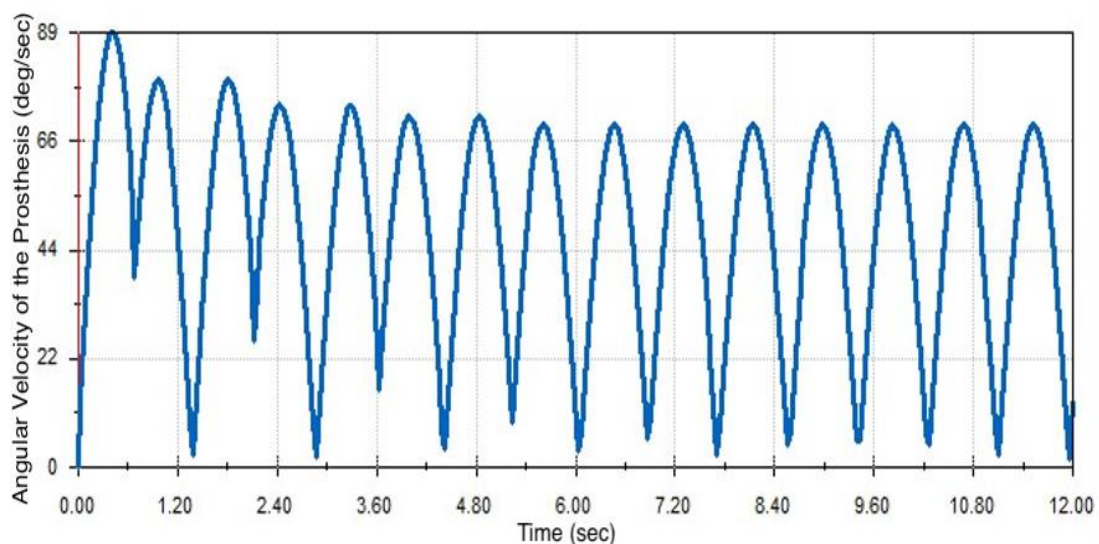
Figure 17: *Angular Velocity of the Prosthesis*

The angular velocity result is shown in Figure 17, and it is seen that the angular velocity can increase from 0 to 90 deg/sec in less than a second. This means the prosthesis can be moved

effortlessly and quickly like a biological leg. According to the graph, it is understood that the prosthesis adapts to the body in about 3 seconds after its first movement from the body.

The angular velocity analyses depicted across Figures 13, 14, and 15 each offer a unique perspective on how the prosthesis behaves in different planes and directions, specifically on the coronal plane. Figure 13 illustrates the angular velocity variation in the x-direction, while Figure 14 provides a visual representation of the variation in the y-direction. Figure 15 extends this analysis by demonstrating how the angular velocity varies with the foot angle in the y-direction, which is also on the coronal plane.

When these detailed, direction-specific analyses are compared with the broader trends shown in Figure 17, some striking similarities and insightful differences emerge. The comprehensive view of Figure 17 suggests the prosthesis can mimic the natural, biological leg's movement by achieving an angular velocity increase from 0 to 90 deg/sec in under a second. This rapid acceleration implies that the prosthesis is capable of fast and effortless movement, adapting to the body in approximately 3 seconds following the initial motion.

However, the patterns observed in Figures 13, 14, and 15 suggest that the velocity variation in the x and y directions on the coronal plane, as well as the angular velocity variation with the foot angle, can be more complex and nuanced. These figures illustrate the critical role of each individual component in contributing to the overall efficiency and performance of the prosthesis, as seen in Figure 17. Therefore, while the prosthesis may adapt quickly in general terms (as per Figure 17), the underlying mechanisms of this adaptation (as shown in Figures 13, 14, and 15) demonstrate the intricate interplay of multiple factors that enable such performance. The analysis of these figures together thus offers a comprehensive understanding of the angular velocity characteristics of the prosthesis, providing valuable insights into its overall performance.
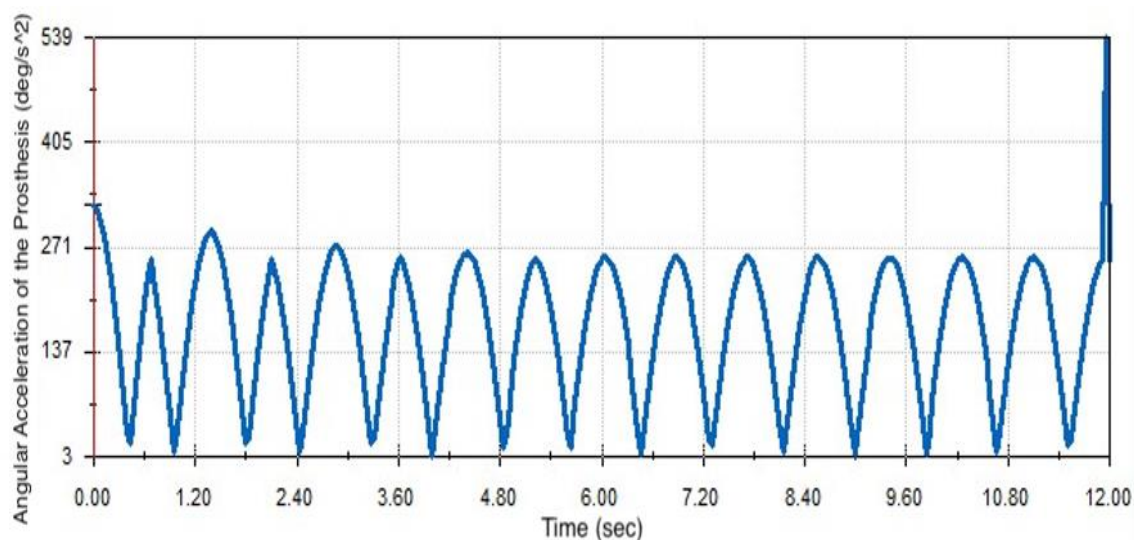
Figure 18: *Angular Acceleration of the Prosthesis*

Considering the angular acceleration result of the prosthesis in Figure 18, the small values and the adaptation to the first movement taken from the body within 2,5 seconds show that the angular progression will be comfortable. From the graph, the fact that there are sharp turns means that daily activities such as running and jumping can be easily performed with this prosthesis.

There is a 'pinpoint' effect towards the end of the 12 seconds movement of the animated model shown in Figure 18. It is because the parts in the assembly are intertwined at any given moment. There is an undesirable separation between the parts while in motion. In this and similar

cases, all the results examined are considered insignificant. (Silver-Thorn, M. B., and Childress, D. S., 1997)
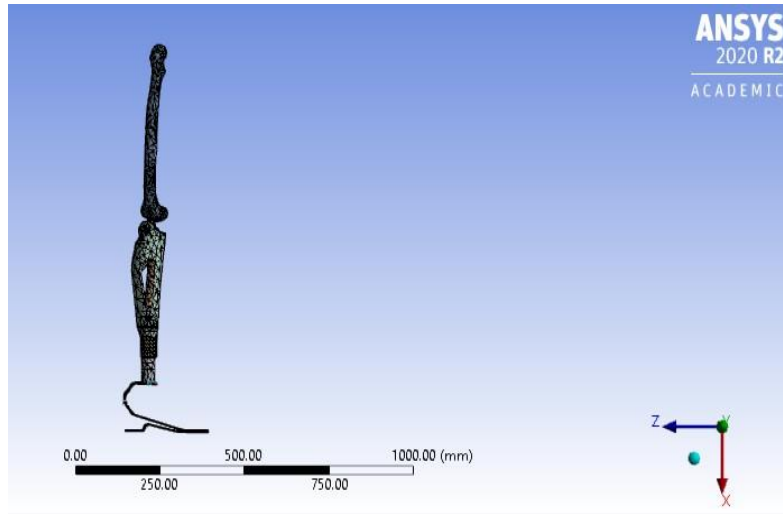
Figure 19: *Position of the assembled model on ANSYS*

The assembled and ready-to-be-analyzed parts are shown in Figure 19. The axis can vary between the files. It should be known whether the axes vary depending on the analysis files. It should be noted that the correct axis must be chosen instead of the global axis coordinates in the analysis section.

Table 1. Material Properties (Tunc, 2022)

Material Properties	Density (kg/m^3)	Young Modulus (MPa)	Poisson Ratio
Cortical Bone	185	17200	0.3
Ti-6Al-4V	4620	96000	0.36

Table 1 shows the material assignments processed in the ANSYS Workbench program and the properties of these materials used. Cortical bone material was defined as the femur bone, and Titanium alloy was defined as the entire prosthesis.

Table 2. Mesh Properties in the model

Mesh Properties	Minimum	Standard Deviation	Average	Maximum
Skewness	0.0068438	0.24022	0.59544	1
Element Quality	0.025853	0.24041	0.54852	1

Mesh properties in Table 2 were obtained without any changes after mesh settings. Considering the general anatomical modeling integrity, there is a need for an artificial system that will allow the knee to bending movement since there are no patella and ligaments. While making contact definitions, the boundary conditions between the parts that will make angular movements have been made by considering the abovementioned situations.

In the definitions on the model, it is presumed that an average person is 80 kg, and considering the personal information such as muscle, fat, and bone in the body, a safety factor of approximately 1.3 is used to calculate a body with the gravity effect as 80 kg x 9.81 m/s^2 x 1.27 = 1000 N is considered to be. According to the mechanics of materials calculations, if the body is considered 2D, 1000 N is provided to carry a force of 500 N to each leg when the force distribution is made by coming and separating each. That is also known as bedding on the same axis with

multiple parts. The 500 N is defined from the femoral head on the hip. The program theoretically defines it so that the kneecap can be moved with a frictionless and limited angle for rotation in the y direction where it should be. In the foot part, a contact definition is made without friction and not allowing separation.
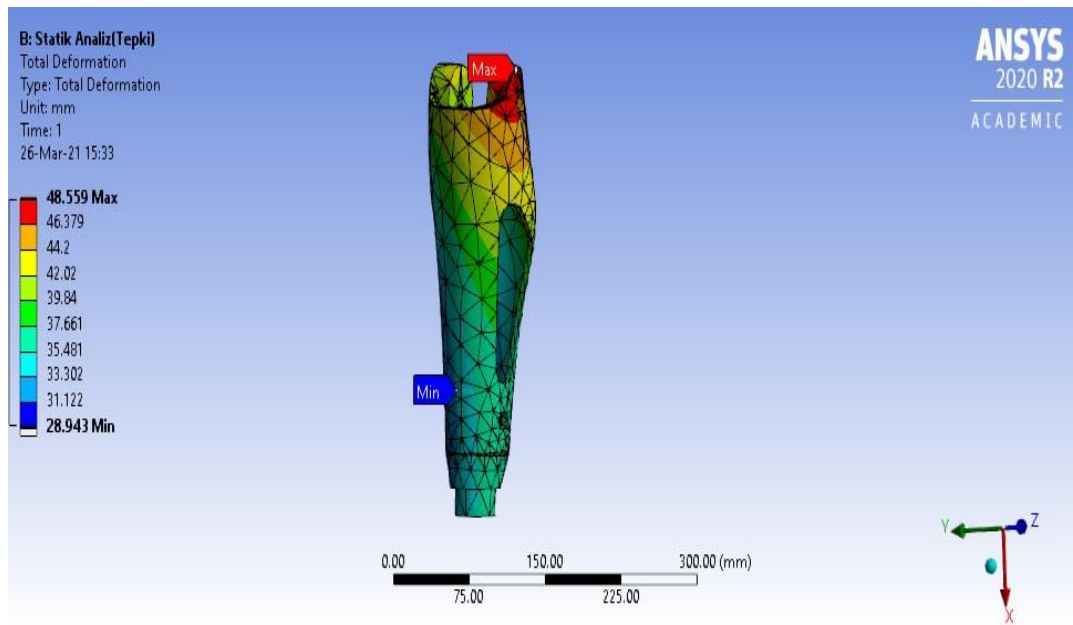
Figure 20: Total deformation for the prosthesis in the model

The prosthesis shown in Figure 20 is made for the right leg, is forced to turn outward with each step, and is colored with a red zone. 40 - 45 mm range defines that.
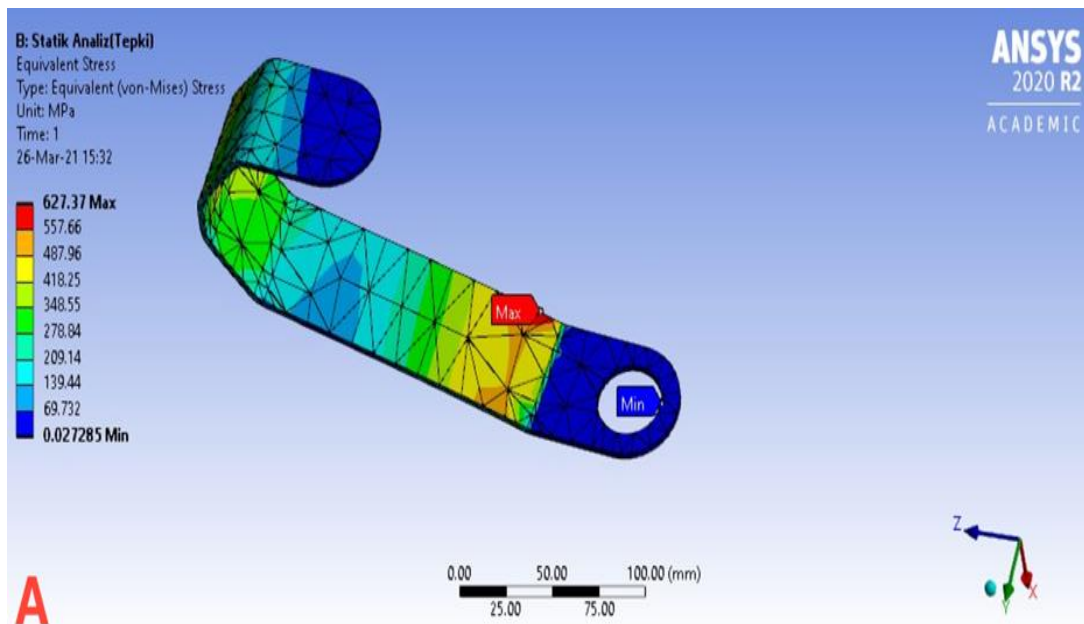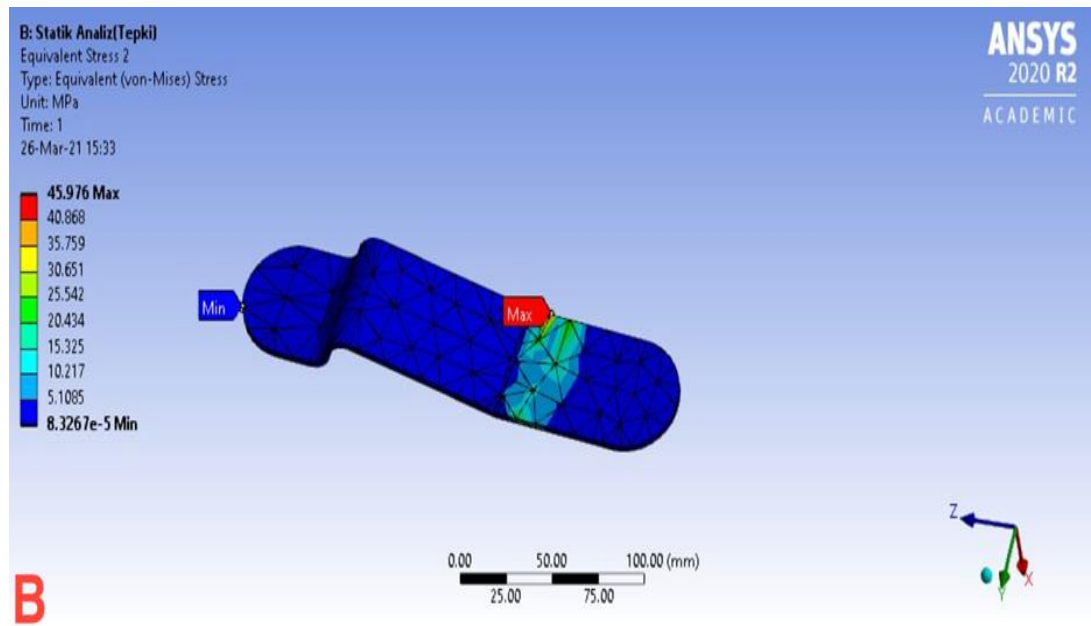
Figure 21: *Von–Mises stresses the artificial foot defined for model A) The upper part of the foot. B) The lower part of the foot.*

As seen in Figure 21a, the stresses vary between 200-600 MPa. To confirm the solutions on Workbench, the force input value was 500 N. From hip to toe, the diameter changes in some sections, increasing the total load on these sections. In Figure 21b, the stresses are low, as expected. The results show that the prosthesis can carry the body. (Verim et al., 2010; Fukaya et al., 2018; Rony et al., 2020)

3. DISCUSSION AND CONCLUSION

Table 3. Displaying angular values in Solidworks-Literature-MATLAB

	Prosthesis Angular Velocity (deg/sec)	Prosthesis Angular Acceleration (deg/sec^2)
Literature	*-400 – 400*	*-4000 – 4000*
MATLAB	*(47 - 52) (ω_x)* *(-676) – (-510) (ω_y)*	*(-330) – (-71)*
Solidworks	*0 – 90*	*0 - 338*

Table 3 shows the resolved result ranges of the values important in the solution of the kinematic equation used in this study. That indicates whether they are within the lower and upper limits in the literature. Although the methods used to find the knee's angular velocity and acceleration values vary according to the literature, the obtained results and the theoretically accepted values are very close, as in Table 3. This also sheds light on the accuracy of the study.

Values may be too small for the lower and upper bounds at first. However, factors such as iteration limits and approximation methods used for mathematical analysis in programs have an effect, and these are dependent on the programs; that is, the user does not have the opportunity to intervene. When these results are considered by participating in the whole walking cycle, it is expected to give results close to reality. Of course, the values such as weight and length used for the solution in this study, omission, and assumptions were made to facilitate the solution of the equation. Naturally, they deviate from the dynamic solution that should be obtained. (Zachariah,

S. G., and Sanders, J. E., 2000; Zhang, M., and Roberts, C., 2000; Wang, Z. and Li, H., 2005; Anon, 2018)

An attempt has been made to develop a method for calculating the knee disarticulation prosthesis and the loads on this prosthesis. Similar results were obtained in different computer programs (MATLAB, Solidworks, and ANSYS Workbench) that support each other. Model-based and equation-based analysis, different differential equation-solving methods, and the computer features' capacity also affect the solution time. In terms of the results obtained, when compared with the results in the literature, overall solution integrity was achieved. As a result of this type of amputation, the solution, and functioning integrity will vary depending on the position of the prosthesis that will serve as an artificial limb and whether it is a single or multi-piece. The mathematical modeling and approaches to be used for the solution will vary. These three programs were used separately to calculate the loads on the prosthesis. The formulas, initial and boundary conditions, assumptions, and omissions applied are all software-based. A method was obtained by using three programs together. The solutions from each program are shown in Table 3.

CONFLICT OF INTEREST

Author(s) approve that to the best of their knowledge, there is no conflict of interest or common interest with an institution/organization or a person that may affect the paper's review process.

AUTHOR CONTRIBUTION

Gürsel ŞEFKAT contributed significantly to the preparation stages before the method, in the calculations, in the literature research, in the implementation of the application, the control of the accuracy of the research and analysis method, and the creation of the general content, structure, and the writing of the article.

İsmet Emircan Tunç made a significant contribution to the establishment, programming, analysis and interpretation of both the MATLAB and ANSYS model of the article subject system.

REFERENCES

1. An, N. (2013). Human Femur Bone. https://grabcad.com/library/human-femur-bone-1 (Erişim Tarihi: 28.03.2022)
2. Anon (2016). Ön çapraz bağ yaralanması. https://bezmialemdragoshastanesi.com/tr/Sayfalar/ortopedi/on-capraz-bag-yaralanmasi.aspx (Erişim Tarihi: 28.03.2022)
3. Anon (2022a). Anatomide hareket terimleri. Vikipedi, Özgür Ansiklopedi. https://tr.wikipedia.org/wiki/Anatomide_hareket_terimleri (Erişim Tarihi: 07.05.2022)
4. Anon (2022b). Kinematics. In Wikipedia, The Free Encyclopedia. https://en.wikipedia.org/w/index.php?title=Kinematics&oldid=1080472428 (Erişim Tarihi: 07.05.2022)
5. Anon (2022c). Femur by Anatomy Next. https://anatomy.app/encyclopedia/femur (Erişim Tarihi: 08.05.2022)
6. AnyBody Technology. (2020, December 7). [Webcast] - Physical stresses on caregivers when repositioning patients in bed [Video]. YouTube. https://www.youtube.com/watch?v=knOfERwrBbI (Erişim Tarihi: 08.05.2022)
7. AnyBody Technology. (2021a, April 8). [Webcast] – Uncertainties on knee ligament properties estimated from laxity measurements [Video]. YouTube. https://www.youtube.com/watch?v=-zoj829VDsk (Erişim Tarihi: 08.05.2022)

8. AnyBody Technology. (2021b, February 19). [Webcast] – AnyBodyRun: A web application for running biomechanics [Video]. YouTube. https://www.youtube.com/watch?v=6zNbbP8XzUk (Erişim Tarihi: 08.05.2022)

9. AnyBody Technology. (2021c, January 18). [Webcast] – Biomechanical investigation of a passive upper extremity exoskeleton for manual handling [Video]. YouTube. https://www.youtube.com/watch?v=HSsvjouKIQQ (Erişim Tarihi: 09.05.2022)

10. AnyBody Technology. (2021d, May 11). [Webcast] – A model-based methodology to predict the biomechanical consequences of tibial inserts [Video]. YouTube. https://www.youtube.com/watch?v=1CVlqJDRNOU (Erişim Tarihi: 09.05.2022)

11. AnyBody Technology. (2022a, January 28). [Webcast] – Investigation of bracing to unload muscle and knee contact forces for knee patients [Video]. YouTube https://www.youtube.com/watch?v=AcFMkJ8IvpI (Erişim Tarihi: 09.05.2022)

12. AnyBody Technology. (2022b, May 06). [Webcast] – The Role of the Anterior Hip Capsule in Daily Hip Performance [Video.] YouTube https://www.youtube.com/watch?v=xnvg7GxUI_Y (Erişim Tarihi: 09.05.2022)

13. Castermans T, Duvinage M, Cheron G, & Dutoit T. Towards Effective Non-Invasive Brain-Computer Interfaces Dedicated to Gait Rehabilitation Systems. *Brain Sciences*. 2014; 4(1):1-48. https://doi.org/10.3390/brainsci4010001

14. Diogo, S. (2012). Prosthetic Leg. https://grabcad.com/library/prosthetic-leg (Erişim Tarihi: 03.04.2022)

15. Joseph C. McCarthy, Philip C. Noble & Richard N. Villar, (2017). *Hip Joint Restoration. Worldwide Advances in Arthoscopy, Arthroplasty, Osteotomy nad Joint Preservation Surgery*. Springer Nature. https://doi.org/10.1007/978-1-4614-0694-5.

16. Lei, Shuangyan & Frank, Matthew & Anderson, Donald & Brown, Thomas, (2014). A Method to Represent Heterogeneous Materials for Rapid Prototyping: The Matryoshka Approach. *Rapid Prototyping Journal*. 20. https://doi.org/10.1108/RPJ-10-2012-0095

17. M. Garrett, T. Kerr, & B. Caulfield, (1999). Phase-Dependent Inhibition of H-Reflexes During Walking in Humans Is Independent of Reduction in Knee Angular Velocity. *Journal of Neurophysiology*, 82(2), 747-753. https://doi.org/10.1152/jn.1999.82.2.747

18. Morrey, B., & Berry, D. (2011). *Joint Replacement Arthroplasty* (4th ed.). Wolters Kluwer.

19. Öncen, H. (2016). Ossa Crucis (Tibia - fibula). https://aduvetfak.wordpress.com/2016/12/26/ossa-cruris-tibia-fibula/ (Erişim Tarihi: 05.03.2022)

20. Rony I., Idsart Kingma, Vosse de Boode, Gert S. Faber, & Jaap H. van Dieën (2020). Angular velocity, moment, and power analysis of the ankle, knee, and hip joints in the goalkeeper's diving save in football. *Frontiers in Sports and Active Living*, 2, 2020, ISSN 2624-9367, doi:10.3389/fspor.2020.00013

21. Silver-Thorn, M. B., & Childress, D. S. (1997). Generic, geometric finite element analysis of the transtibial residual limb and prosthetic socket. *Journal of rehabilitation research and development*, 34(2), 171–186. https://pubmed.ncbi.nlm.nih.gov/9108344/

22. Singh, A. P., (2017). Femur Anatomy and Attachments. https://boneandspine.com/femur-anatomy-and-attachments/ (Erişim Tarihi: 12.05.2022)

23. Takashi Fukaya, Wataru Nakano, Hirotaka Mutsuzaki, & Koichi Mori (2018). Smoothness of the knee joint movement during the stance phase in patients with severe knee osteoarthritis. *Asia-Pacific Journal of Sports Medicine*, 14, 1-5, ISSN 2214-6873, https://doi.org/10.1016/j.asmart.2018.08.002

24. Taylor, T. (2019). Bones of the Leg and Foot. https://www.innerbody.com/anatomy/skeletal/leg-foot (Erişim Tarihi: 15.05.2022)

25. Tunc, I. E. (2022). CT Görüntülü Femur – Tibia Kemiklerinin Katı Modelinden Diz İmplantı Analizi. *Yüzüncü Yıl Üniversitesi Fen Bilimleri Enstitüsü Dergisi*, 27(1), 140-157. https://doi.org/10.53433/yyufbed.1036092

26. Verim Ö., Tasgetiren S., & Öksüz M., (2010). Bilgisayar Destekli Organ Mühendisliği Temel Yaklaşımları. *Biyoteknoloji Elektronik Dergisi*, 1, 27-34. (Erişim Tarihi: 07.05.2022)

27. Wang, Zheng & Li, Haiyun (2005). A novel 3D finite element modeling based on medical images for intervertebral disc biomechanical analysis. Conference proceedings: ... Annual International Conference of the IEEE Engineering in Medicine and Biology Society. IEEE Engineering in Medicine and Biology Society. Conference. 3. 3202-5. https://doi.org/10.1109/IEMBS.2005.1617157

28. Xiaohong Jia, Ming Zhang, & Winson C.C Lee, (2004). Load transfer mechanics between trans-tibial prosthetic socket and residual limb-dynamic effects, *Journal of Biomechanics*, 37 (9), 1371-1377, ISSN 0021-9290, https://doi.org/10.1016/j.jbiomech.2003.12.024

29. Zachariah, S. G., & Sanders, J. E. (2000). Finite element estimates of interface stress in the trans-tibial prosthesis using gap elements are different from those using automated contact. *Journal of Biomechanics*, 33 (7), 895–899. https://doi.org/10.1016/S0021-9290(00)00022-1

30. Zhang, M., & Roberts, C. (2000). Comparison of computational analysis with clinical measurement of stresses on below-knee residual limb in a prosthetic socket. *Medical engineering & physics*, 22(9), 607–612. https://doi.org/10.1016/S1350-4533(00)00079-5

31. Zhang, M., Mak, A. F., & Roberts, V. C. (1998a). Finite element modelling of a residual lower-limb in a prosthetic socket: a survey of the development in the first decade. *Medical engineering & physics,* 20(5), 360–373. https://doi.org/10.1016/s1350-4533(98)00027-7

32. Zhang, M., Turner-Smith, A. R., Tanner, A., & Roberts, V. C. (1998b). Clinical investigation of the pressure and shear stress on the trans-tibial stump with a prosthesis. *Medical engineering & physics*, 20(3), 188–198. https://doi.org/10.1016/s1350-4533(98)00013-7